Published in final edited form as:
J Cereb Blood Flow Metab. 2009 July ; 29(7): 1262–1272. doi:10.1038/jcbfm.2009.47.

Inhibition of NADPH oxidase is neuroprotective after ischemia-reperfusion

Hai Chen, PhD[1,2,3], **Yun Seon Song, PhD**[1,2,3,4], and **Pak H Chan, PhD**[1,2,3]

[1]Department of Neurosurgery, Stanford University School of Medicine, Stanford, California, USA

[2]Department of Neurology and Neurological Sciences, Stanford University School of Medicine, Stanford, California, USA

[3]Program in Neurosciences, Stanford University School of Medicine, Stanford, California, USA

[4]College of Pharmacy, Sookmyung Women's University, Seoul, Republic of Korea

Abstract

NADPH oxidase (NOX) is well-known as a major source for superoxide radical generation in leukocytes. Superoxide radicals play a significant role in brain ischemia-reperfusion (I/R) injury. Recent data have also revealed expression of NOX in the brain. However, how NOX is involved in pathological processes after cerebral ischemia remains unknown. Therefore, we subjected mice deficient in the NOX subunit gp91^{phox} (gp91^{phox}–/–), those treated with the NOX inhibitor apocynin, and wild-types to 75 mins of focal ischemia followed by reperfusion. At 24 h of reperfusion, the gp91^{phox}–/– and apocynin-treated mice exhibited 50% less brain infarction, as well as 70% less cleaved spectrin compared with the wild-types. The levels of 4-hydroxy-2-nonenal, malondialdehyde, and 8-hydroxy-2'-deoxyguanosine increased significantly after I/R, indicating oxidative brain injury. NOX inhibition reduced biomarker generation. Furthermore, NOX was involved in post-ischemic inflammation in the brains, as less intercellular adhesion molecule-1 upregulation and less neutrophil infiltration were found in the NOX-inhibited mice following I/R. Moreover, gp91^{phox} expression increased after ischemia, and was further aggravated by genetic copper/zinc-superoxide dismutase (SOD1) ablation, but ameliorated in SOD1-overexpressing mice. The present study suggests that NOX plays a role in oxidative stress and inflammation, thus contributing to ischemic brain injury.

Keywords

apocynin; focal ischemia; gp91^{phox}; NADPH oxidase; oxidative stress; superoxide dismutase

Introduction

Reactive oxygen species (ROS) play an important role in cerebral ischemia-reperfusion (I/R) damage (Chan, 1996, 2001). During reperfusion, robust oxidants are generated and are directly involved in damage to cellular macromolecules such as lipids, proteins, and nucleic acids, eventually leading to cell death (Chan, 2001).

Correspondence: Dr PH Chan, Neurosurgical Laboratories, Stanford University, 1201 Welch Rd, MSLS #P314, Stanford, CA 94305-5487, USA. Phone: 650-498-4457; fax: 650-498-4550. E-mail: phchan@stanford.edu.

Disclosure/Conflict of Interest
None

Many prooxidant enzymes, including nitric oxide synthase, cyclooxygenase, and xanthine oxidase, participate in oxidative injury in cerebral ischemia (Chan, 2001). NADPH oxidase (NOX) is originally found in leukocytes and is a major resource of ROS generation in leukocytes (Lambeth, 2004). NOX is a multisubunit complex composed of membrane-associated $gp91^{phox}$ and $p22^{phox}$ subunits and cytosolic subunits, including $p47^{phox}$, $p67^{phox}$, and $p40^{phox}$. As NOX is activated, cytosolic subunits $p47^{phox}$, $p67^{phox}$, and $p40^{phox}$ translocate into membranes and fuse with catalytic subunit $gp91^{phox}$. The activated enzyme complex transports electrons to oxygen, thus producing superoxide anion ($O_2^{\cdot -}$), a precursor of ROS (Bedard and Krause, 2007).

Recent studies have also suggested that NOX is expressed in the central nervous system (Bedard and Krause, 2007). *In vitro* studies have revealed NOX expression in neurons, astrocytes, and microglia (Bedard and Krause, 2007). Immunohistochemistry studies have demonstrated that NOX subunits are widely distributed in the cortex, hippocampus, and cerebellum *in vivo* (Infanger *et al*, 2006; Kim *et al*, 2005). Genetic ablation of the $gp91^{phox}$ subunit reduced brain infarction by 46% at 22 h of reperfusion after 2 h of focal ischemia (Walder *et al*, 1997). However, these studies failed to reveal how NOX contributes to ischemic brain damage. In this study, we focused on the role of NOX in post-ischemic oxidant generation and inflammation progression. In addition to prooxidant enzymes, antioxidant enzymes are also robustly expressed in the brain (Chan, 2001). Copper/zinc-superoxide dismutase (SOD1) is one of the most important antioxidant enzymes and is crucial for reducing oxidant stress after cerebral I/R. SOD1 knockout (KO) mice are more susceptible to focal ischemia challenge (Kondo *et al*, 1997). However, cross-talk between the oxidant-generation enzyme NOX and the antioxidant enzyme SOD1 after cerebral ischemia remains unknown.

In this study, we used both genetic $gp91^{phox}$ ablation and the NOX inhibitor apocynin to investigate the role of NOX in cerebral I/R damage. We found that inhibition of NOX alleviated oxidative stress and reduced the inflammation process after cerebral focal ischemia, and subsequently protected the brain against I/R damage. In addition, we found that cerebral I/R causes upregulation of the NOX subunit $gp91^{phox}$ and that post-ischemic $gp91^{phox}$ overexpression was regulated by the level of endogenous SOD1.

Materials and methods

Animal Preparation

gp91 KO mice that were developed and maintained in the C57BL/6J strain were purchased from the Jackson Laboratory (Bar Harbor, ME, USA) and were characterized earlier (Pollock *et al*, 1995). SOD1-deficient mice, including SOD1 heterozygous (SOD1−/+) and SOD1 KO mice, designated CD1-SOD1<tm1 Cje>, were produced by Epstein *et al* (Kondo *et al*, 1997). SOD1 transgenic (TG) mice of the SOD1 TGHS/SF-218 strain were derived from the founder stock previously described (Epstein *et al*, 1987). No phenotypic differences were observed among the gp91 KO and wild-type (WT) mice or the SOD1 TG, SOD1 KO, and WT mice. Mouse genotypes were determined by a PCR of DNA from tail biopsies. Male adult mice (25–30 g) were anesthetized with 5% isoflurane for induction and 1.0% isoflurane vaporized in N_2O and O_2 (3:2) for maintenance. Rectal temperatures were monitored and maintained at 37.0°C ± 0.5°C with a homeothermic blanket control unit (Harvard Apparatus, Holliston, MA, USA). Artery blood samples were taken and analyzed for blood gas and electrolytes before and during middle cerebral artery occlusion (MCAO) using an i-STAT analyzer (East Windsor, NJ, USA).

Focal Cerebral Ischemia Models in Mice

Focal cerebral ischemia was induced in the mice by occlusion of the left MCA using a 6–0 coated suture as described before (Chen *et al*, 2005). Briefly, the left common carotid artery was exposed and the external carotid artery (ECA) was dissected distally. The internal carotid artery (ICA) was isolated and a coated suture (6–0 monofilament nylon) was introduced into the ECA lumen and then gently advanced into the ICA lumen to block MCA blood flow. A successful occlusion was indicated by a decrease in regional cerebral blood flow (CBF) to less than 20% of the baseline. After 75 mins of MCAO, CBF was restored by suture withdrawal. The incision was closed and the mice recovered under a heating lamp. The animals were divided into three groups: WT, apocynin-treated, and gp91 KO. Prior to apocynin treatment, preliminary studies were done using various doses and an optimal dose was chosen. Thus, for apocynin treatment, 4 mg/kg (Sigma-Aldrich, St. Louis, MO, USA) were administered by intra-peritoneal injection (ip) 5 mins before suture withdrawal. In our pilot experiments, there was no significant difference in brain infarction between WT and vehicle-treated mice (0.25 ml normal saline, ip). In addition, for better comparison between the WT and gp91 KO mice, we used WT mice without vehicle treatment in this study. All animal procedures used in this study were conducted in strict compliance with the NIH Guide for the Care and Use of Laboratory Animals, and approved by Stanford University's Administrative Panel on Laboratory Animal Care.

Regional Cerebral Blood Flow Measurement

Changes in regional CBF at the surface of the left cortex were recorded using a blood flow monitor (Laserflo BMP^2; Vasamedics, Eden Prairie, MN, USA) with a fiber optic probe. The tip of the probe was over the core area supplied by the MCA (2 mm posterior and 6 mm lateral from the bregma). Changes in CBF after MCAO were expressed as a percentage of the baseline value.

Examination of Neurological Symptoms

The mice were examined for neurological deficits at 3 and 24 h of reperfusion after MCAO using a modified five-point scale as reported: *grade 0*, no observable neurological deficit (normal); *grade 1*, flexion of contralateral torso and forelimb upon lifting of the animal by the tail (mild); *grade 2*, circling to the contralateral side but normal posture at rest (moderate); *grade 3*, leaning to contralateral side at rest (severe); *grade 4*, no spontaneous motor activity (very severe) (Bederson *et al*, 1986; Yang *et al*, 1994).

Measurement of Infarct Volume

After 24 and 72 h of reperfusion, the mice were anesthetized and then decapitated. Coronal sections were cut into 2-mm slices using a mouse-brain matrix (Zivic Instruments, Pittsburgh, PA, USA), and were immediately immersed in 2% 2,3,5-triphenyltetrazolium chloride (TTC; Sigma-Aldrich) for 20 mins. The infarction area in each section was calculated with NIH image analysis software. The infarct areas of each slice were separately summed and multiplied by the interval thickness to obtain infarct volumes as described before (Chen *et al*, 2005).

Western Blotting

Whole-cell fractions were obtained from the entire MCA territory (ischemic and non-ischemic sides). Tissues were lysed by lysis buffer (Cell Signaling Technology, Danvers, MA, USA), followed by 30 sec of sonication at 4°C with an ultrasonic processor (VC 130 PB; Sonic & Materials Inc, Newtown, CT, USA). Protein concentration was determined by a bicinchoninic acid method. Equal amounts of samples were loaded per lane and were then electrophoretically separated on SDS gels. The resolved proteins were electrophoretically transferred to a PVDF membrane. The primary antibodies were an anti-α-spectrin antibody (1:5000; Millipore,

Billerica, MA, USA), an anti-cyclooxygenase-2 (COX-2) antibody (1:1000; Cayman, Ann Arbor, MI, USA), an anti-gp91^{phox} antibody (1:1000; BD Bioscience, Franklin Lakes, NJ, USA), an anti-mouse intercellular adhesion molecule-1 (ICAM-1) (1:1000; Biolegend, San Diego, CA, USA), and an anti–β-actin antibody (1:20,000; Sigma-Aldrich). Western blotting was performed with horseradish peroxidase-conjugated secondary IgG (Cell Signaling Technology) with the use of enhanced chemiluminescence detection reagents. Quantitative expression of the proteins was analyzed by scanning the films of the blots and calculating the intensity as measured by Quantity One software (Bio-Rad, Hercules, CA, USA).

Immunohistological Staining

For immunohistochemistry after I/R, the mice were perfused with heparin in saline (2 IU/L), followed by 4% paraformaldehyde. The brains were postfixed in 4% paraformaldehyde overnight, and subsequently cryoprotected with 20% and 30% sucrose. The brains were cut into coronal sections (30 μm) on a freezing microtome (SM 2000R; Leica, Nussloch, Germany). Two coronal sections (0.98 mm anterior and 1.06 mm posterior to bregma) were selected and processed for immunohistological staining. The sections were probed with an antibody against 8-hydroxy-2'-deoxyguanosine (8-OHdG) (1:400; GeneTex, San Antonio, TX, USA) and an anti-4-hydroxy-2-nonenal (HNE) antibody (1:400; Alpha Diagnostic International, San Antonio, TX, USA). The sections were incubated with biotinylated anti-goat IgG (1:400; Vector Laboratories, Burlingame, CA, USA) and avidin-peroxidase (Vector Laboratories). Color reaction was developed with a diaminobenzidine kit (Vector Laboratories). For a negative control, a consecutive section was treated with similar procedures, except that the primary antibody was omitted. Images were observed and captured with a Zeiss optical microscope (Axioplan2). 8-OHdG–positive cells were counted and averaged in four subsequent areas at each section as described before (Franklin and Paxinos, 1997; McColl *et al*, 2007).

Malondialdehyde Detection

Intracellular malondialdehyde (MDA) is a biomarker for lipid peroxidation. After I/R, MDA levels in ischemic and contralateral hemispheres were measured using a Bioxytech LPO-586 assay kit (OxisResearch, Foster City, CA, USA) according to the manufacturer's instructions. MDA concentration was calculated by measuring the absorbance at 586 nm on a spectrophotometer (Molecular Devices, Sunnyvale, CA, USA), using N-methy-2-phenylindole as a substrate.

Myeloperoxidase Measurement

Myeloperoxidase (MPO) is an active enzyme expressed in neutrophils and involved in phagocytic lysis of engulfed foreign particles. After I/R, MPO levels in ischemic and nonischemic hemispheres were measured with a Mouse MPO ELISA kit (Hycult Biotechnology, Uden, The Netherlands) according to the manufacturer's instructions. Samples were measured on a spectrophotometer (Molecular Devices) at 586 nM and the MPO concentration was calculated with a standard curve according to the manufacturer's instructions.

Quantification and Statistical Analysis

The data are expressed as mean ± SEM. Comparison between groups was achieved with ANOVA using the Fisher PLSD test. Significance was accepted at $P<0.05$ (StatView; Adept Scientific Inc, Acton, MA, USA).

Results

NOX Inhibition Reduced Brain Infarction after I/R

Physiological parameters showed no significant differences in arterial blood gas and electrolytes between the groups. The preischemic physiological values were as follows (WT and gp91 KO mice, respectively): 146±24 and 132±10 PaO_2; 39±2.4 and 43±5.8 $PaCO_2$; pH 7.38±0.03 and 7.39±0.05; Na 146±0.6 and 145±0.3 mmol/l; K 4.3±0.4 and 4.6±0.2 mmol/l (n = 3–5). During ischemia, the physiological values were as follows: 130±10 and 112±6 PaO_2; 45±4 and 39±4 $PaCO_2$; pH 7.34±0.02 and 7.4±0.09; Na 147±1.1 and 146±1.7 mmol/l; K 4.2±0.3 and 5.0±0.7 mmol/l (n = 3–5).

To investigate the role of NOX in ischemic brain damage, infarction volume was assessed in the WT, apocynin-treated, and gp91 KO brains after I/R. The average infarction volume in the WT mice was 53.9±8.6 mm^3 after 75 mins of focal ischemia and 24 h of reperfusion (Figure 1A and 1C). The predominant lesion was found in a region 4–6 mm posterior to the frontal pole where the blood supply is primarily from the MCA. In the apocynin-treated and gp91 KO mice, infarction volume was significantly less than in the WT mice (24.9±6.9 mm^3 and 26.0 ±4.8 mm^3, apocynin-treated and gp91 KO, respectively, P<0.05, Figure 1A and 1C). We further measured the brain infarct at 72 h of reperfusion after ischemia. Similarly, larger infarction tissue was observed in the WT mice than in the apocynin-treated and gp91 KO mice (106.2±12.5 mm^3, 57.7±15.8 mm^3, and 52.0±11.8 mm^3, respectively, P<0.05, Figure 1B and 1D). The difference in brain infarction among the WT, apocynin-treated, or gp91 KO mice is not likely due to the cerebral vascular change after NOX inhibition, because brain blood flow dropped to a similar level among the three groups during ischemia (12%–14.6%, P>0.05, Figure 1E and 1F).

NOX Inhibition Ameliorated Cleaved Spectrin and Improved Neurological Function after I/R

To study the cellular mechanism of brain damage, we examined cleaved spectrin after I/R. Spectrin is a cytoskeletal protein that lines the intracellular side of the plasma membrane, forming a scaffolding and maintaining plasma membrane integrity. Cleaved spectrin can cause cytoskeleton destruction and bleb formation in the cell membrane, ultimately degrading cells and leading to cell death (Büki *et al*, 2000).

We used a spectrin antibody which recognizes both caspase (150 and 120 kDa) and calpain (150 kDa) cleaved products to assess brain injury after I/R. At 3 h of reperfusion, a large amount of cleaved spectrin products (150 kDa) was found in the WT mice. The ratio of spectrin density between the ipsilateral and contralateral sides in the WT mice was ~2.4, which is significantly higher than in the apocynin-treated and gp91 KO mice (1.24–1.45, P<0.05, Figure 2A and 2C). Only very limited cleaved spectrin products were revealed at 120 kDa by the same blot (1.08–1.14, Figure 2A and 2C). At 24 h of reperfusion, pronounced cleaved spectrin products (both 150 and 120 kDa) were found in WT brain tissue (~2.30, ~1.92; 150 and 120 kDa, respectively, Figure 2B and 2D). If apocynin was present, cleaved spectrin products were reduced (~1.40, ~1.08; 150 kDa and 120 kDa, respectively, P<0.05, Figure 2B and 2D). The gp91 KO mice also showed less cleaved spectrin compared with the WT mice (~1.36, ~1.1; 150 and 120 kDa, respectively, P<0.05, Figure 2B and 2D). These data suggest that NOX activity contributed to cleaved spectrin after cerebral I/R.

We then investigated whether NOX inhibition improved neurological function after I/R. At 3 h of reperfusion, the animals exhibited prominent neurological deficits, with no significant differences in neurological-deficit scores among the WT, apocynin-treated, and gp91 KO groups (P>0.05, Figure 2C). However, after 24 h of reperfusion, the average neurological-deficit score for the WT mice was ~2.8, which was significantly higher than in the apocynin-

treated or gp91 KO mice (1.9–2.0, $P<0.05$, Figure 2E). These data indicate that mice subjected to NOX inhibition not only had less ischemic infarct but also maintained better neurological function.

NOX Inhibition Alleviated Oxidative Stress *In Vivo* after I/R

We examined the role of NOX in post-ischemic oxidative injury in mouse brains by measuring the lipid peroxidation products HNE and MDA. Low HNE immunoactivity was detected in the contralateral hemisphere (data not shown). However, a number of HNE-positive cells were observed on the ipsilateral side of the WT brains at 24 h of reperfusion after focal ischemia (Figure 3A). After NOX inhibition, there were fewer HNE-positive cells in the ischemic brains compared with the WT mice (Figure 3A). We also measured the concentration of MDA in brain tissue. In the contralateral hemisphere, there was no significant difference in MDA concentration among the WT, apocynin-treated, and gp91 KO mice, indicating similar baseline conditions (111–130 pmol/mg protein, Figure 3B). After I/R, MDA generation was increased by ~1.5-fold in the ipsilateral brains of the WT animals compared with the contralateral side, and was significantly higher than in the apocynin-treated and gp91 KO mice (0.97–1.07-fold, $P<0.05$, Figure 3B).

DNA oxidative damage was assessed by immunohistological staining using an 8-OHdG antibody. 8-OHdG, an oxidized nucleoside of DNA and an indicator of a DNA oxidative lesion, was not detected in the contralateral hemisphere (data not shown). We also did not find 8-OHdG–positive cells at 3 h of reperfusion (Figure 3D). In contrast, a significant amount of 8-OHdG–positive cells was observed on the ipsilateral side of the WT brains at 24 h of reperfusion after focal ischemia ($69.2 \pm 8.1/0.15$ mm^2, Figure 3D and 3E). 8-OHdG immunoactivity was not as prominent in the apocynin-treated and gp91 KO mice as in the WT mice ($33.4 \pm 7.8/0.15$ mm^2, $32.7 \pm 12.3/0.15$ mm^2, $P<0.05$, Figure 3D and 3E).

NOX and the Inflammation Process after I/R

Significant cerebral inflammation occurs after cerebral ischemia and it may exacerbate brain damage (Danton and Dietrich, 2003). To further characterize the role of NOX in the post-ischemic pathological process, especially inflammation progress, we examined expression of ICAM-1, which is an intercellular interaction molecule and mediates neutrophils recruited into the brain parenchyma. Western blotting revealed minimal ICAM-1 expression in the contralateral hemisphere (Figure 4A). After ischemia and 24 h of reperfusion, ICAM-1 expression increased ~1.8-fold in the WT ipsilateral hemisphere compared with the contralateral side, and upregulation of ICAM-1 in the WT mice was significantly higher than in the apocynin-treated and gp91 KO mice (~1.1-fold, $P<0.05$, Figure 4B). We then detected neutrophil infiltration by measuring the concentration of the neutrophil-specific enzyme MPO in brain. In the contralateral hemisphere, MPO concentration was low and there was no significant difference among the WT, apocynin-treated, and gp91 KO mice (2.8–3.2 ng/mg protein, Figure 4B). At 24 h of reperfusion, MPO concentration increased to ~8.2 ng/mg protein in the WT ipsilateral hemisphere, which suggests neutrophil infiltration. In the apocynin-treated and gp91 KO groups, MPO increase was significantly less than in the WT mice (3.5–3.7 ng/mg protein, $P<0.05$, Figure 4C). Lastly, we detected COX-2 expression after I/R. All three groups showed similar levels of COX-2 upregulation (1.6–1.8-fold increase compared with the contralateral side) in the ipsilateral hemisphere after focal ischemia ($P>0.05$, Figure 4D and 4E).

Cross-talk between NOX and SOD1

To study the interaction between the prooxidant enzyme NOX and the antioxidant enzyme SOD1, we examined gp91^{phox} expression in the WT, SOD1 KO, and SOD1 TG mice after focal ischemia. After ischemia, a significant increase in gp91^{phox} protein was found, especially

at 1 h of reperfusion (Figure 5A and 5B). However, the amount of $gp91^{phox}$ in the SOD1 TG mice was much less than in the WT mice after focal ischemia (*P<0.05, Figure 5A and 5B). Furthermore, we compared $gp91^{phox}$ expression among the WT, SOD1−/+, and SOD1 KO mice after mild ischemia (30 mins), because of the high sensitivity of SOD1 KO to prolonged ischemia. We did not find significant differences between the WT and SOD1−/+ mice (P>0.05, Figure 5C and 5D). However, in the SOD1 KO mice, there was significantly more $gp91^{phox}$ upregulation than in the WT mice after focal ischemia at 1 and 4 h of reperfusion (*P<0.05, Figure 5C and 5D).

Discussion

Inhibition of NOX is Neuroprotective in Ischemic Damage

The present study demonstrates that genetic ablation of $gp91^{phox}$ or pharmacological inhibition of NOX reduced brain infarction by ~53% after 75 mins of ischemia and 24 h of reperfusion. This was further proved by less cleaved spectrin in mouse brains subjected to NOX inhibition. To further examine whether NOX inhibition indeed protects the brain or just delays the progress of brain damage after ischemia, we measured infarction volume in the mice at 72 h of reperfusion after focal ischemia. The brains showed more infarction volume than at 24 h, which suggests a delayed cell death process. The gp91 KO or apocynin-treated mice still showed 46%–50% less brain infarction than the WT mice at 72 h of reperfusion. Taken together, these data suggest that inhibition of NOX is neuroprotective after cerebral ischemia. In addition, the spectrin antibody, which recognizes cleaved spectrin products by both caspase (150 and 120 kDa) and calpain (150 kDa), was used to assess brain injury after I/R. Cleaved spectrin has been reported in a variety of cerebral pathological conditions, including traumatic brain injury (TBI) and brain focal ischemia (Copin *et al*, 2005; Deng-Bryant *et al*, 2008). Oxidative stress plays an important role in the process of cleaving spectrin, because oxidative stress causes Ca^{2+} homeostasis disturbance, which induces calpain-mediated cleavage of spectrin (Deng-Bryant *et al*, 2008). Indeed tempol, a catalytic scavenger of free radicals, not only attenuated protein nitration but also inhibited cleavage of spectrin after TBI (Deng-Bryant *et al*, 2008). In addition, EUK-134, a synthetic superoxide dismutase and catalase mimetic, prevented oxidative stress and cleaved spectrin after kainate intracerebral injection *in vivo* (Rong *et al*, 1999). In our study, Western blotting revealed both 150- and 120-kDa products at 24 h of reperfusion, although only 150-kDa cleaved products were detected at 3 h of reperfusion. Therefore, we postulate that at early reperfusion (3 h), the calpain pathway is already activated and can subsequently cause cell necrosis (Lipton, 1999). In contrast, both calpain-mediated necrosis and caspase-mediated apoptosis play a role in ischemic brain damage at late reperfusion (24 h) (Lipton, 1999). Consistent with our findings, previous studies reported that active caspase-3 exhibited a significant increase at 24 h of reperfusion, but not at 6 h of reperfusion after MCAO (Wang *et al*, 2008). We also detected a 2–2.3-fold larger infarction volume at 3 days than at 24 h of reperfusion, which indicates a continuous evolution of cell death, leading to delayed larger infarction. More studies are required to determine which cell death signal pathways contribute to delayed brain cell death.

In addition to neutrophils, recent data have identified that NOX also expresses on neurons, microglia, and astrocytes constitutively, where it may function as in physiological redox signals (Bedard and Krause, 2007). We hypothesize that NOX activation in brain tissue can contribute to oxidant generation and subsequent brain damage *in vivo* after cerebral focal ischemia. *In vitro* studies demonstrated a large amount of $O_2^{\cdot -}$ generation and significant cell death in cultured neurons with glucose deprivation and glucose reperfusion (GD/GR) treatment (Suh *et al*, 2007). Inhibition of NOX by $p47^{phox}$ subunit ablation can abolish GD/GR-induced $O_2^{\cdot -}$ production and prevent neuronal death (Suh *et al*, 2007). Apocynin can also reduce $O_2^{\cdot -}$ generation in cultured neurons subjected to oxygen-glucose deprivation treatment (Suh

et al, 2008). We observed a significant amount of lipid or DNA peroxidation products, including MDA, HNE, and 8-OHdG, at 24 h of reperfusion in the WT mice. In addition, we observed fewer HNE and MDA products and less DNA oxidation in the gp91 KO and apocynin-treated mice. Moreover, we found that NOX inhibition by apocynin reduced $O_2^{\cdot -}$ generation in mouse brains at 3 h of reperfusion using a hydroethidine injection *in vivo* (data not shown). Taken together, these data support the view that inhibition of NOX reduces free radical generation and alleviates brain oxidative damage, subsequently reducing brain infarction *in vivo*.

Alleviation of Post-ischemic Inflammation Progress after NOX Inhibition

There is substantial evidence that inflammation occurs following focal cerebral ischemia and that it is implicated as a secondary injury mechanism (Danton and Dietrich, 2003). Cerebral post-ischemic inflammation is characterized by upregulation of inflammation mediators and infiltration of inflammatory cells such as neutrophils and microglia in the ischemic brain (Barone and Feuerstein, 1999). Recruitment of neutrophils into brain parenchyma is initiated by both chemoattractants within the brain and by binding to adhesion molecules (such as ICAM-1) on the surface of endothelial cells. Previous reports demonstrated that neutrophils infiltrated into post-ischemic brain parenchyma as early as 6 h and that neutrophil infiltration can cause detrimental effects through reocclusion of the microvasculature, producing ROS and releasing more proinflammatory mediators such as tumor necrosis factor-α, and interleukin-1β, thus potentially amplifying the cellular inflammatory response (Danton and Dietrich, 2003; Wang *et al*, 2007; Weston *et al*, 2007). Mice that have neutrophil immunodepletion demonstrated a 3.0-fold decrease in infarct volume, reduced neurological deficit, and less mortality compared with controls after 2 h of focal ischemia and 24 h of reperfusion (Connolly *et al*, 1996). In our study, significantly less MPO expression was found in the apocynin-treated and gp91 KO mice, which indicates less neutrophil accumulation after NOX inhibition. ICAM-1 is constitutively expressed in the endothelium of brain microvascular structure at low concentrations. After cerebral ischemia, it is upregulated by cytokines and binds β2 integrins on neutrophils, thus mediating neutrophil adhesion and transmigration into brain parenchyma (Frijns and Kappelle, 2002; Panés *et al*, 1999). Knockout of ICAM-1 caused a degree of brain protection similar to neutrophil depletion in a focal ischemia model (Connolly *et al*, 1996). We found that ICAM-1 upregulation was less significant in the gp91 KO and apocynin-treated mice than in the WT mice at 24 h of reperfusion. This further strengthened our hypothesis that NOX inhibition reduces neutrophil infiltration after cerebral ischemia. Taken together, our data suggest that in addition to reducing oxidant stress, NOX inhibition can also protect against cerebral damage by alleviating inflammation processes such as neutrophil infiltration. In our study, NOX inhibition failed to inhibit expression of the inflammation-induced protein COX-2. This suggests that ICAM-1 upregulation and neutrophil infiltration is mediated by NOX instead of COX-2–mediated pathways. We speculate that NOX activation mediates the inflammation process through changes in the redox state in the brain after ischemia. Oxidative stress plays an important role in the regulation of the post-ischemic neuro-inflammation process. Gene expression studies have demonstrated that after ischemia, an increase in oxygen radicals triggers expression of a number of pro-inflammatory genes that are regulated by the redox-sensitive transcription factor, nuclear factor-kappa-B (Chan, 2001; Song *et al*, 2007). Nevertheless, the molecules and pathways that are activated by NOX and mediate changes in post-ischemic inflammation need further elucidation.

Apocynin is a commonly used NOX inhibitor with relatively low affinity (IC50 ~10 μM) in neutrophils (Simons *et al*, 1990). Apocynin inhibits the release of $O_2^{\cdot -}$ through NOX by blocking migration of $p47^{phox}$ to the membrane, thus interfering with assembly of the functional NOX complex (Touyz, 2008). It was reported that apocynin needs MPO activation to form a dimer before inhibiting $p47^{phox}$ translocation (Heumüller *et al*, 2008). In cells that

are not rich in MPO, apocynin can reduce oxidant stress through a non-specific oxidative scavenger effect instead of NOX inhibition (Heumüller *et al*, 2008). However, besides MPO, other peroxidases such as horseradish peroxidase can also induce an apocynin dimer formation with a consequent NOX inhibitory effect (Touyz, 2008; Vejrazka *et al*, 2005). In addition, *in vivo* studies demonstrated that MPO secreted by neutrophils can be taken up by endothelial cells, where apocynin can then be metabolized to active dimers, thus inhibiting vascular cell NOX (Touyz, 2008). Our study revealed an ~3-fold increase in MPO concentration after ischemia in the WT mice. Thus, we speculate that apocynin acted as an NOX inhibitor either through MPO generated by neutrophils or through peroxidase, although the direct scavenger effect of apocynin needs to be further examined. In addition, the gp91 KO mice also showed a protective effect similar to that seen with apocynin treatment, which strengthens our conclusion that inhibition of NOX is neuroprotective after cerebral ischemia. It was reported that apocynin improved the outcome in MCAO at a low dosage (2.5 mg/kg iv), but increased intracerebral hemorrhage at 5 mg/kg (Tang *et al*, 2008). This could be due to the longer ischemia period (120 mins) and larger infarction (~140 mm^3) in that study. Thus, the mice were less tolerant to apocynin. Furthermore, apocynin was administered intravenously and the absorption was faster and more complete (Tang *et al*, 2008). We administered apocynin 5 mg/kg ip, and no significant side effect was observed.

Cross-talk between SOD1 and NOX after Cerebral Ischemia

Our results show that $gp91^{phox}$ expression is increased after focal ischemia. In agreement with our view, upregulation of gp91 mRNA and protein was also reported in other studies such as that using a rat focal ischemia model (Kusaka *et al*, 2004). We further investigated cross-talk between the prooxidant enzyme NOX and the antioxidant enzyme SOD1. SOD1 is an important endogenous cytosolic antioxidant enzyme (Chan, 2001). The SOD1 TG mice, which have a 2.3-fold overexpression of SOD1 in brain tissue, exhibited 40% less brain infarct and edema, as well as less $O_2^{\cdot -}$ generation in the brain than the WT mice after I/R (Epstein *et al*, 1987; Kinouchi *et al*, 1991; Noshita *et al*, 2002). In contrast, generation of more $O_2^{\cdot -}$ and exacerbation of neuronal death were revealed in the SOD1−/+ mice with a 50% decrease in SOD1 activity after global ischemia (Kawase *et al*, 1999). Our results show that the SOD1 KO mice have a 1.8 −2.8-fold greater increase in $gp91^{phox}$ than the WT mice after focal ischemia. This suggests that NOX expression is regulated by the redox state of brain tissue and that oxidative stress contributes to NOX upregulation in brain tissue. To further strengthen our hypothesis, we tested $gp91^{phox}$ expression in the SOD1 TG mice after focal ischemia. Indeed, we found that $gp91^{phox}$ upregulation after cerebral ischemia is less pronounced in SOD1 TG mice than in WT mice. Therefore, NOX activity can itself be potentially subjected to feedforward regulation after SOD1 mutation. In addition to antioxidant-ability deficit, the SOD1 KO mice exhibited more significant NOX upregulation, which generates more endogenous $O_2^{\cdot -}$, thereby amplifying progress of brain injury after focal ischemia. In contrast, less vulnerability to ischemic insult in the SOD1 TG mice is attributed to both higher SOD1 levels and less $O_2^{\cdot -}$ generated by NOX. Moreover, we found that apocynin administration reduced infarction by more than 50% in manganese-superoxide dismutase KO mice after 30 mins of ischemia and 72 h of reperfusion (unpublished data). This further suggests the elaborate cross-talk between NOX and SOD and that inhibition of NOX can be a new therapeutic target for antioxidant-enzyme deficit.

In conclusion, the results from both pharmacological inhibition and genetic ablation studies show that NOX contributes to ischemic cerebral damage, through increasing oxidant generation and aggravation of the inflammation process. In addition, NOX expression is regulated by the redox state after cerebral ischemia. Our findings further stress the important role of NOX in brain ischemic damage.

Acknowledgments

This work was supported by grants P50 NS014543, RO1 NS025372, RO1 NS036147, and RO1 NS038653 from the National Institute of Neurological Disorders and Stroke. The content is solely the responsibility of the authors and does not necessarily represent the official views of the NINDS or the National Institutes of Health. We thank Liza Reola and Bernard Calagui for technical assistance and Cheryl Christensen for editorial assistance.

References

Barone FC, Feuerstein GZ. Inflammatory mediators and stroke: new opportunities for novel therapeutics. J Cereb Blood Flow Metab 1999;19:819–834. [PubMed: 10458589]

Bedard K, Krause K-H. The NOX family of ROS-generating NADPH oxidases: physiology and pathophysiology. Physiol Rev 2007;87:245–313. [PubMed: 17237347]

Bederson JB, Pitts LH, Tsuji M, Nishimura MC, Davis RL, Bartkowski H. Rat middle cerebral artery occlusion: evaluation of the model and development of a neurologic examination. Stroke 1986;17:472–476. [PubMed: 3715945]

Büki A, Okonkwo DO, Wang KKW, Povlishock JT. Cytochrome c release and caspase activation in traumatic axonal injury. J Neurosci 2000;20:2825–2834. [PubMed: 10751434]

Chan PH. Role of oxidants in ischemic brain damage. Stroke 1996;27:1124–1129. [PubMed: 8650725]

Chan PH. Reactive oxygen radicals in signaling and damage in the ischemic brain. J Cereb Blood Flow Metab 2001;21:2–14. [PubMed: 11149664]

Chen H, Luo J, Kintner DB, Shull GE, Sun D. Na^+-dependent chloride transporter (NKCC1)-null mice exhibit less gray and white matter damage after focal cerebral ischemia. J Cereb Blood Flow Metab 2005;25:54–66. [PubMed: 15678112]

Connolly ES Jr, Winfree CJ, Springer TA, Naka Y, Liao H, Yan SD, Stern DM, Solomon RA, Gutierrez-Ramos J-C, Pinsky DJ. Cerebral protection in homozygous null ICAM-1 mice after middle cerebral artery occlusion. Role of neutrophil adhesion in the pathogenesis of stroke. J Clin Invest 1996;97:209–216. [PubMed: 8550836]

Copin J-C, Goodyear M-C, Gidday JM, Shah AR, Gascon E, Dayer A, Morel DM, Gasche Y. Role of matrix metalloproteinases in apoptosis after transient focal cerebral ischemia in rats and mice. Eur J Neurosci 2005;22:1597–1608. [PubMed: 16197500]

Danton GH, Dietrich WD. Inflammatory mechanisms after ischemia and stroke. J Neuropathol Exp Neurol 2003;62:127–136. [PubMed: 12578222]

Deng-Bryant Y, Singh IN, Carrico KM, Hall ED. Neuroprotective effects of tempol, a catalytic scavenger of peroxynitrite-derived free radicals, in a mouse traumatic brain injury model. J Cereb Blood Flow Metab 2008;28:1114–1126. [PubMed: 18319733]

Epstein CJ, Avraham KB, Lovett M, Smith S, Elroy-Stein O, Rotman G, Bry C, Groner Y. Transgenic mice with increased Cu/Zn-superoxide dismutase activity: animal model of dosage effects in Down syndrome. Proc Natl Acad Sci USA 1987;84:8044–8048. [PubMed: 2960971]

Franklin, KBJ.; Paxinos, G. The Mouse Brain in Stereotaxic Coordinates. San Diego: Academic Press, Inc; 1997.

Frijns CJM, Kappelle LJ. Inflammatory cell adhesion molecules in ischemic cerebrovascular disease. Stroke 2002;33:2115–2122. [PubMed: 12154274]

Heumüller S, Wind S, Barbosa-Sicard E, Schmidt HHHW, Busse R, Schröder K, Brandes RP. Apocynin is not an inhibitor of vascular NADPH oxidases but an antioxidant. Hypertension 2008;51:211–217. [PubMed: 18086956]

Infanger DW, Sharma RV, Davisson RL. NADPH oxidases of the brain: distribution, regulation, and function. Antioxid Redox Signal 2006;8:1583–1596. [PubMed: 16987013]

Kawase M, Murakami K, Fujimura M, Morita-Fujimura Y, Gasche Y, Kondo T, Scott RW, Chan PH. Exacerbation of delayed cell injury after transient global ischemia in mutant mice with CuZn superoxide dismutase deficiency. Stroke 1999;30:1962–1968. [PubMed: 10471451]

Kim MJ, Shin K-S, Chung Y-B, Jung KW, Cha CI, Shin DH. Immunohistochemical study of $p47^{Phox}$ and $gp91^{Phox}$ distributions in rat brain. Brain Res 2005;1040:178–186. [PubMed: 15804439]

Kinouchi H, Epstein CJ, Mizui T, Carlson E, Chen SF, Chan PH. Attenuation of focal cerebral ischemic injury in transgenic mice overexpressing CuZn superoxide dismutase. Proc Natl Acad Sci USA 1991;88:11158–11162. [PubMed: 1763030]

Kondo T, Reaume AG, Huang T-T, Carlson E, Murakami K, Chen SF, Hoffman EK, Scott RW, Epstein CJ, Chan PH. Reduction of CuZn-superoxide dismutase activity exacerbates neuronal cell injury and edema formation after transient focal cerebral ischemia. J Neurosci 1997;17:4180–4189. [PubMed: 9151735]

Kusaka I, Kusaka G, Zhou C, Ishikawa M, Nanda A, Granger DN, Zhang JH, Tang J. Role of AT_1 receptors and NAD(P)H oxidase in diabetes-aggravated ischemic brain injury. Am J Physiol Heart Circ Physiol 2004;286:H2442–H2451. [PubMed: 15148062]

Lambeth JD. NOX enzymes and the biology of reactive oxygen. Nat Rev Immunol 2004;4:181–189. [PubMed: 15039755]

Lipton P. Ischemic cell death in brain neurons. Physiol Rev 1999;79:1431–1568. [PubMed: 10508238]

McColl BW, Rothwell NJ, Allan SM. Systemic inflammatory stimulus potentiates the acute phase and CXC chemokine responses to experimental stroke and exacerbates brain damage via interleukin-1- and neutrophil-dependent mechanisms. J Neurosci 2007;27:4403–4412. [PubMed: 17442825]

Noshita N, Sugawara T, Hayashi T, Lewén A, Omar G, Chan PH. Copper/zinc superoxide dismutase attenuates neuronal cell death by preventing extracellular signal-regulated kinase activation after transient focal cerebral ischemia in mice. J Neurosci 2002;22:7923–7930. [PubMed: 12223545]

Panés J, Perry M, Granger DN. Leukocyte-endothelial cell adhesion: avenues for therapeutic intervention. Br J Pharmacol 1999;126:537–550. [PubMed: 10188959]

Pollock JD, Williams DA, Gifford MAC, Li LL, Du X, Fisherman J, Orkin SH, Doerschuk CM, Dinauer MC. Mouse model of X-linked chronic granulomatous disease, an inherited defect in phagocyte superoxide production. Nat Genet 1995;9:202–209. [PubMed: 7719350]

Rong Y, Doctrow SR, Tocco G, Baudry M. EUK-134, a synthetic superoxide dismutase and catalase mimetic, prevents oxidative stress and attenuates kainate-induced neuropathology. Proc Natl Acad Sci USA 1999;96:9897–9902. [PubMed: 10449791]

Simons JM, Hart BA, Ip Vai, Ching TR, Van Dijk H, Labadie RP. Metabolic activation of natural phenols into selective oxidative burst agonists by activated human neutrophils. Free Radic Biol Med 1990;8:251–258. [PubMed: 2160411]

Song YS, Lee Y-S, Narasimhan P, Chan PH. Reduced oxidative stress promotes NF-κB-mediated neuroprotective gene expression after transient focal cerebral ischemia: lymphocytotrophic cytokines and antiapoptotic factors. J Cereb Blood Flow Metab 2007;27:764–775. [PubMed: 16868554]

Suh SW, Gum ET, Hamby AM, Chan PH, Swanson RA. Hypoglycemic neuronal death is triggered by glucose reperfusion and activation of neuronal NADPH oxidase. J Clin Invest 2007;117:910–918. [PubMed: 17404617]

Suh SW, Shin BS, Ma H, Van Hoecke M, Brennan AM, Yenari MA, Swanson RA. Glucose and NADPH oxidase drive neuronal superoxide formation in stroke. Ann Neurol 2008;64:654–663. [PubMed: 19107988]

Tang XN, Cairns B, Cairns N, Yenari MA. Apocynin improves outcome in experimental stroke with a narrow dose range. Neuroscience 2008;154:556–562. [PubMed: 18511205]

Touyz RM. Apocynin, NADPH oxidase, and vascular cells. A complex matter. Hypertension 2008;51:172–174. [PubMed: 18086948]

Vejrazka M, Mícek R, Stípek S. Apocynin inhibits NADPH oxidase in phagocytes but stimulates ROS production in non-phagocytic cells. Biochim Biophys Acta 2005;1722:143–147. [PubMed: 15716123]

Walder CE, Green SP, Darbonne WC, Mathias J, Rae J, Dinauer MC, Curnutte JT, Thomas GR. Ischemic stroke injury is reduced in mice lacking a functional NADPH oxidase. Stroke 1997;28:2252–2258. [PubMed: 9368573]

Wang Q, Tang XN, Yenari MA. The inflammatory response in stroke. J Neuroimmunol 2007;184:53–68. [PubMed: 17188755]

Wang Y, Luo J, Chen X, Chen H, Cramer SW, Sun D. Gene inactivation of Na^+/H^+ exchanger isoform 1 attenuates apoptosis and mitochondrial damage following transient focal cerebral ischemia. Eur J Neurosci 2008;28:51–61. [PubMed: 18662334]

Weston RM, Jones NM, Jarrott B, Callaway JK. Inflammatory cell infiltration after endothelin-1-induced cerebral ischemia: histochemical and myeloperoxidase correlation with temporal changes in brain injury. J Cereb Blood Flow Metab 2007;27:100–114. [PubMed: 16736051]

Yang G, Chan PH, Chen J, Carlson E, Chen SF, Weinstein P, Epstein CJ, Kamii H. Human copper-zinc superoxide dismutase transgenic mice are highly resistant to reperfusion injury after focal cerebral ischemia. Stroke 1994;25:165–170. [PubMed: 8266365]

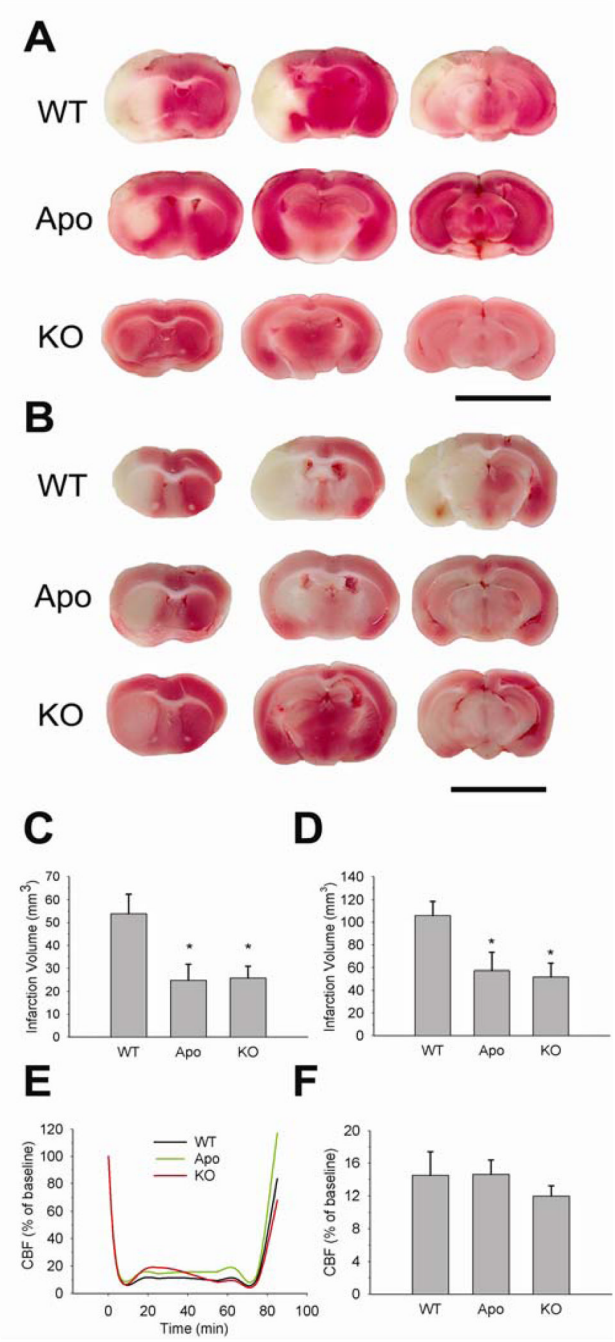

Figure 1.

Decreased brain infarct volume after I/R in mice with NOX inhibition. Representative photographs of TTC staining at 24 h **(A)** and 72 h **(B)** of reperfusion after MCAO. Scale bars = 1 cm. (**C**) Infarct volume at 24 h of reperfusion after MCAO in WT, apocynin-treated (Apo), and gp91 KO mice (**P*<0.05 vs. WT mice, *n* =5–11). WT mice showed larger brain infarct volume than apocynin-treated and gp91 KO mice. (**D**) Infarct volume at 72 h of reperfusion after MCAO in WT, apocynin-treated, and gp91 KO mice (**P*<0.05 vs. WT mice, *n* =5–6). WT mice exhibited larger brain infarct than apocynin-treated and gp91 KO mice. (**E**) Representative changes in CBF level during MCAO among WT, apocynin-treated, and gp91

KO mice. (**F**) Summarized data of CBF decrease in WT, apocynin-treated, and gp91 KO mice during ischemia ($P>0.05$, $n = 4–11$).

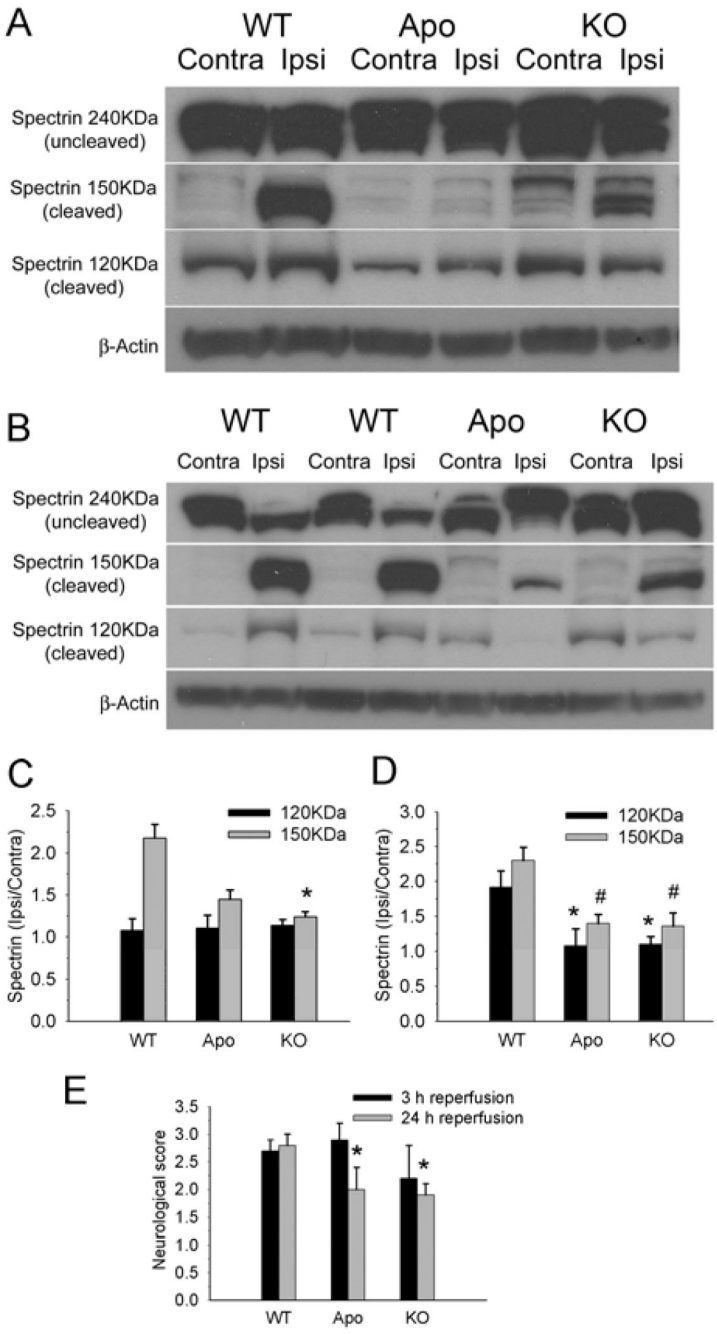

Figure 2.

Cleaved spectrin and neurological deficit scores in WT, apocynin-treated (Apo), and gp91 KO mice. (**A**) Western blot analysis of cleaved spectrin at 3 h of reperfusion. Significant cleaved spectrin products (150 kDa) were detected in the WT mice, but not in the apocynin-treated and gp91 KO mice. Contra, contralateral; Ipsi, ipsilateral. (**B**) Western blot analysis of cleaved spectrin at 24 h of reperfusion. NOX inhibition reduced cleaved spectrin products (both 150 and 120 kDa). (**C**) Summarized data from (**A**). **P*<0.05 vs. WT spectrin (150 kDa), *n* =6. Summarized data are presented as a ratio of (cleaved spectrin/uncleaved spectrin)/β-actin, which are normalized to the contralateral side. (**D**) Summarized data from (**B**). **P*<0.05 vs. WT spectrin (120 kDa); #*P*<0.05 vs. WT spectrin (150 kDa), *n* =4–6. Summarized data are

presented as described in **(C)**. (**E**) Neurological deficit score measurement at 3 and 24 h of reperfusion. NOX inhibition had no significant effect on post-ischemic neurological deficit scores at 3 h of reperfusion, However, at 24 h of reperfusion, the neurological deficit scores in the WT mice were significantly higher than in the apocynin-treated and gp91 KO mice **P*<0.05 vs. WT mice at 24 h of reperfusion, *n* =7–16.

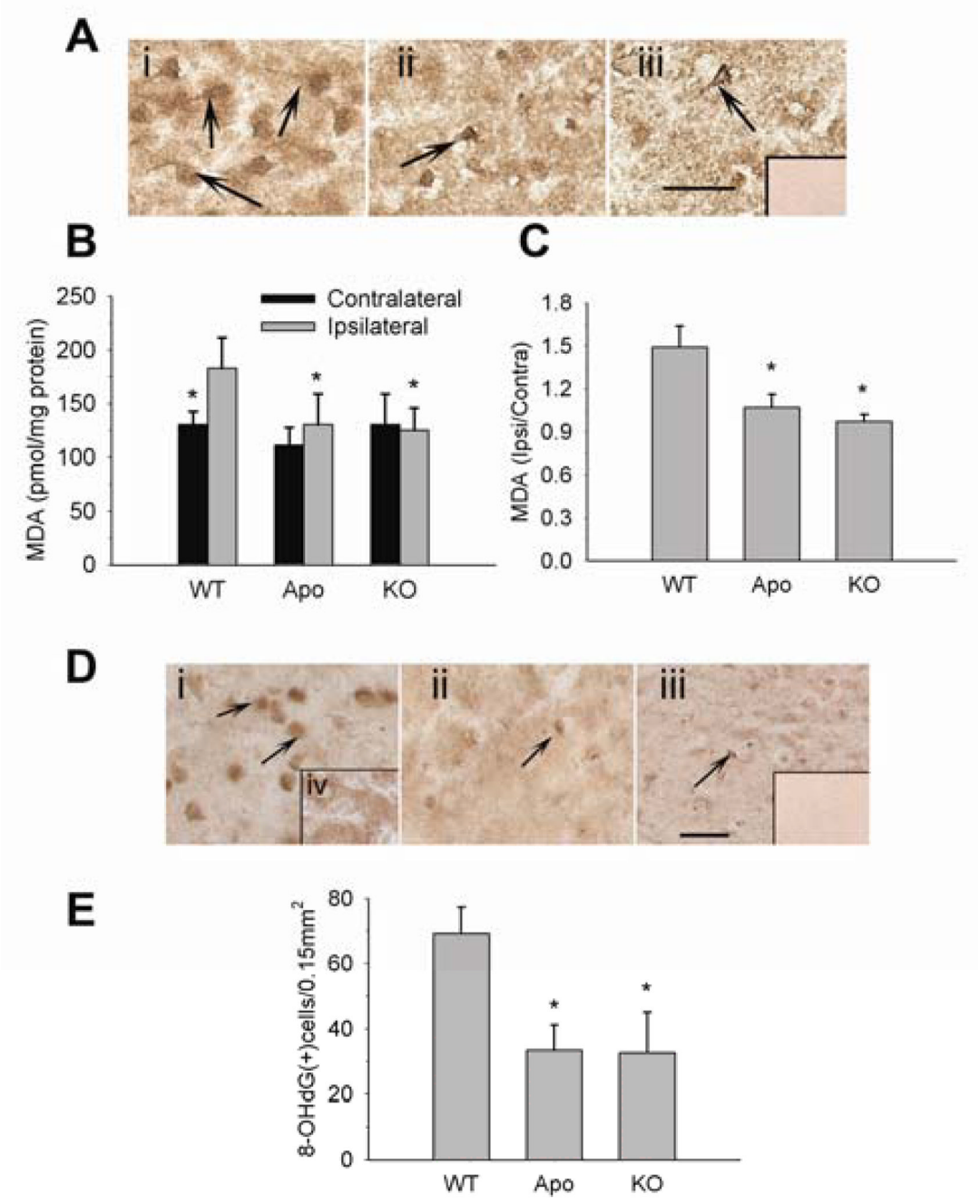

Figure 3.

NOX inhibition reduced lipid and DNA peroxidation products after focal ischemia. (**A**) At 24 h of reperfusion, more HNE-positive cells were detected in the WT ipsilateral hemisphere than in the apocynin-treated and gp91 KO mice. (**i**) WT ipsilateral; (**ii**) apocynin-treated ipsilateral; (**iii**) gp91 KO ipsilateral. Arrows, positive-stained cells. Inset, Negative control. Scale bar = 50 μm. Images shown are representative of 4–5 experiments. (**B**) MDA concentration in mouse brains after ischemia. MDA was produced in the WT ipsilateral hemisphere (**P*<0.05 vs. WT ipsilateral side, *n* =4–5). (**C**) MDA concentration ratio as ipsilateral/contralateral. MDA level was significantly less in the apocynin-treated (Apo) and gp91 KO mice compared with the WT mice (**P*<0.05 vs. WT mice, *n* =4–5). (**D**) At 24 h of reperfusion, 8-OHdG immunoactivity

was more prominent in the WT ischemic hemisphere than in the apocynin-treated and gp91 KO mice. (**i**) WT mice ipsilateral; (**ii**) apocynin-treated mice ipsilateral; (**iii**) gp91 KO mice ipsilateral; (**iv**) WT mice ipsilateral. **(i, ii, iii)** 24 h of reperfusion, **(iv)** 3 h of reperfusion. Arrows, positive-stained cells. Inset, Negative control. Scale bar = 50 μm. Images shown are representative of 4–5 experiments. (**E**) Summarized data from **(D)**. More 8-OHdG-positive cells were seen in the WT groups (**P*<0.05 vs. WTmice *n* = 4–5).

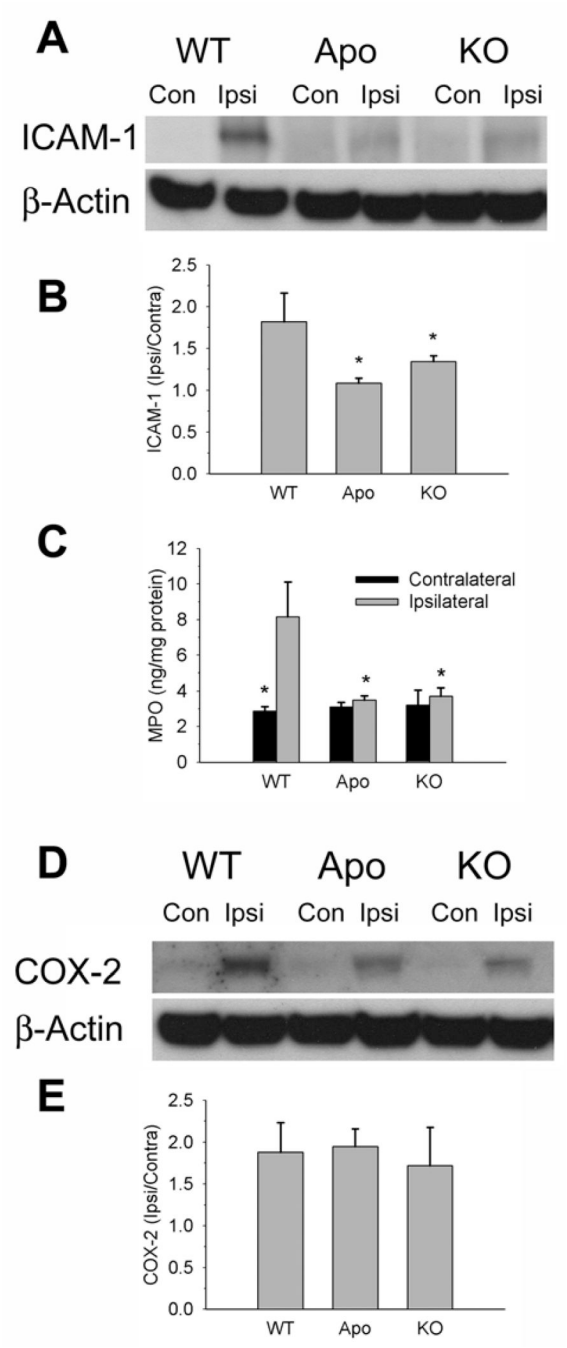

Figure 4.

NOX inhibition alleviated the progress of cerebral post-ischemic inflammation. (**A**) Western blot analysis of ICAM-1 expression following I/R. I/R induced ICAM-1 upregulation in the mouse brains. Con, contralateral; Ipsi, ipsilateral. (**B**) Summarized data from (**A**) are presented as a ratio of ICAM-1/β-actin, which are normalized to the contralateral side. (**P*<0.05 vs. WT mice). **(C**) ELISA analysis of MPO content in WT, apocynin-treated (Apo), and gp91 KO mice. In the ipsilateral hemisphere, MPO concentration was significantly higher in the WT group than in the apocynin-treated or gp91 KO mice (**P*<0.05 vs. WT ipsilateral side, *n* =4–6). (**D**) Western blot analysis of COX-2 expression following I/R. COX-2 expression increased in the mouse brains after I/R. (**E**) Summarized data from (**D**) are presented as a ratio of COX-2/

β-actin, which are normalized to the contralateral side. There were no significant differences in COX-2 expression among the WT, apocynin-treated, and gp91 KO mice following I/R ($P>0.05$, $n=3–5$).

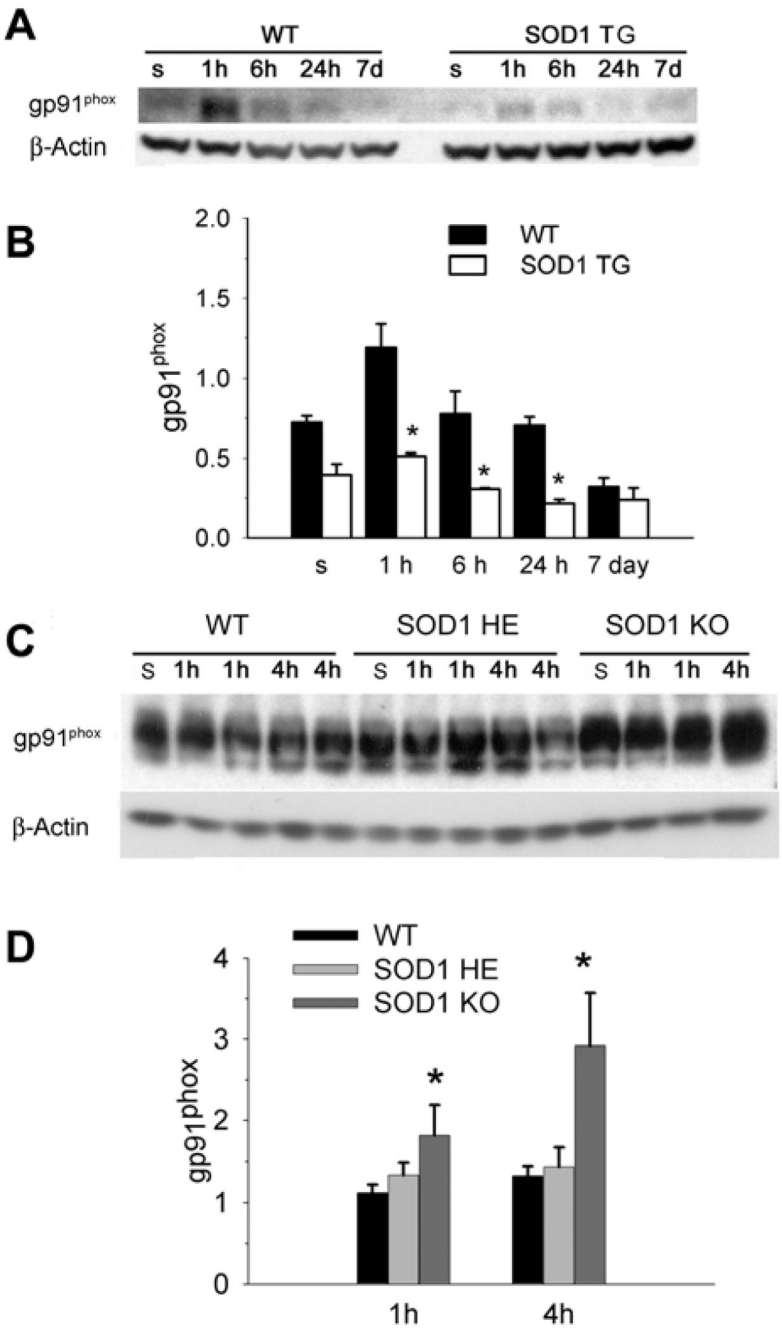

Figure 5.

Cross-talk between NOX and SOD1 after focal ischemia. (**A**) Decreased levels of gp91^{phox} expression in the SOD1 TG mouse brains compared with the WT brains after 30 mins of MCAO. s, sham (**B**) Summarized data from (**A**) (*P<0.05 vs. WT mice at the same time points, n =3). (**C**) In the SOD1 KO mice, gp91^{phox} levels were significantly increased at 1 and 4 h compared with the WT or heterozygous (HE) mice after focal ischemia. (**D**) Summarized data from (**C**) (*P<0.05 vs. SOD1 WT mice, n =4).